Journal of Wood Science

ORIGINAL ARTICLE

Effect of face-layer moisture content and face–core–face ratio of mats on the temperature and vapor pressure behavior during hot-pressing of wood-based panel manufacturing

Kazushige Murayama[1][*] , Kensuke Kukita[2], Hikaru Kobori[2], Yoichi Kojima[2], Shigehiko Suzuki[3] and Kohta Miyamoto[1]

Abstract

Wood-based panels are made by consolidating mats of resinous wooden raw materials under a hot-pressing process. This study investigates the effect of face-layer moisture content (MC) and face–core–face (FCF) ratio of mats on the temperature and vapor pressure behavior during the hot-pressing process. Raising the face-layer MC and lowering the face-layer thickness was expected to reduce the time of reaching 100 °C in the hot-pressing process. When the temperature rise was limited or the core temperature decreased after reaching 100 °C (defined as plateau in this study), the mats with 25% and 30% face-layer MC with 1:2:1 FCF ratio reached the highest plateau core temperature, but required a longer time to complete the plateau. The relationship between core plateau temperature and maximum core vapor pressure was well described by the Antoine equation, which empirically models the vapor pressure as a function of temperature. The Antoine equation held across both face-layer MC series (varying face-layer MC at constant FCF ratio) and FCF series (varying FCF ratio at constant face-layer MC). The mat with 20% face-layer MC and 1:2:1 FCF ratio reached 180 °C within the shortest time, regardless of the evaluation conditions.

Keywords: Wood-based panels, Temperature behavior, Vapor pressure behavior, Hot-pressing, Face-layer moisture, Face–core–face ratio

Introduction

Wood-based panels are generally manufactured by consolidating mats of resinated wooden raw materials (for example; strands, particles, or fibers) under a hot-pressing process [1–3]. Hot-pressing is a critical process that not only determines the physical and mechanical properties of wood-based panels [4–7], but also affects the energy consumption and costs on the production line

[8–10]. Hot-pressing induces complex and dynamic phenomena viz., heat transfer, mass transfer (mainly moisture vaporization and vapor flow), resin curing, and mat densification within the consolidating mat [1–3, 9, 11]. During hot-pressing, heat is conducted from the heated platen to the mat surfaces [9, 12]. As a result, it vaporizes the surface moisture from the mat. The generated vapor pressure increases with temperature. As the vapor pressure differs between the core and surfaces of the mat, the vapor transfers from the surfaces to the core [9, 12, 13]. By convection, the hot vapor flow causes temperature increments inside the mat. Once the mat temperature has reached the local boiling point of water, the

*Correspondence: kazumura039@ffpri.affrc.go.jp
[1] Forestry and Forest Products Research Institute, 1 Matsunosato, Tsukuba, Ibaraki 305-8687, Japan
Full list of author information is available at the end of the article

Murayama *et al. J Wood Sci* (2021) 67:42

Page 2 of 10

vaporization is accelerated, and the vapor flows horizontally and escapes from the mat edges. At this time, the rate of the temperature rise stagnates because most of the heat is utilized in the phase change. After a limited temperature rise, the mat temperature gradually increases as heat is conducted from the hot platen because the moisture content (MC) inside the mats decreases [9, 12]. The temperature rise causes thermosetting resin curing and the hydrothermal effect causes mass densification [4, 9, 10, 12, 14]. Therefore, understanding the heat and mass transfer mechanism is important for clarifying the complex physical phenomena inside the mat during hot-pressing.

To understand the heat and mass transfers inside the mat, many researchers have measured the temperature and vapor pressure behavior during hot-pressing. Some studies have reported that the core temperature rises more rapidly in mats with a larger initial MC than in drier mats [8, 12, 15, 16]. Moreover, a high mat MC limits the rise period of the core temperature. The same effect of mat MC was observed in mats with a high aspect ratio or mats formed from dense raw material [12, 17]. Furthermore, when the mat density is high, the rates of core temperature rise and maximum core vapor pressure (VP_{max}) increase [8, 15–18], and the core temperature rises more slowly in thicker mats than in thinner mats [8, 16, 17]. Raising the platen temperature and shortening the press closing time has been shown to accelerate the core temperature rise and increase the VP_{max} during hot-pressing [8, 12, 15–17]. Other researchers have developed mathematical models describing the core temperature and vapor pressure behaviors during hot-pressing. For example, Dai et al. [19] developed a simulation model that generally agrees with the measured core temperature and vapor pressure behavior. However, they reported that mat properties such as conductivity and permeability must be experimentally characterized in further study. Hence, investigating the temperature and vapor pressure during hot-pressing by both experimental and simulation approaches is still important.

The effect of mat moisture gradient on the mat temperature and vapor pressure remains under-investigated. As is widely known, spraying water on the mat surfaces (steam shock method) or spraying vapor from the mat surfaces to the core (steam injection method) accelerates the temperature rise in the mat [15, 20]. Steam shock and steam injection improve the convective heat transfer. For the same reason, a high face-layer MC should enhance the heat transfer to the core-layer of the mat. The present study evaluates the thickness effect of face-layers with higher MC than the core-layer. As the heat transfer generally increases through woods with higher MC, we considered that the face–core–face (FCF) ratio

under the optimum condition would improve the rate of temperature rise. Therefore, this study aimed to investigate the effect of face-layer MC and FCF ratio of the mat on the temperature and vapor pressure behaviors during hot-pressing. Specifically, it establishes the relationship between each index and the total MC of the mat.

The results of this study are expected to further our understanding of heat and mass transfer during the hot-pressing of mats in wood-based panel manufacture. The ultimate goal is to optimize the performance and production of wood-based panels.

Materials and methods

In this study, sugi (*Cryptomeria japonica*) strands were used for making lab-scale wood-based panels (see Fig. 1). The average dimensions of 900 strands are 15 mm length, 2.9 mm width, and 0.18 mm thickness. This element may reduce voids in the mats due to its dimensions and the fact that it is a low-density softwood material. Therefore, we chose this element because we think that it is easy to observe the effect of vapor pressure and temperature on different MC mats. The strands (with an initial MC of approximately 5%) were conditioned by water-spraying, and were placed at room temperature for over seven days inside plastic bags. The target MC of the strands was varied as 10, 12.5, 15, 20, 25, and 30%. The target and measured MCs differed within 1% under all conditions. MC of the mats configures a wide range, which is beyond the current industrial production conditions, because this study aims to understand the temperature and vapor pressure behavior of mats of wide range MC. The mats were hand-formed into three layers (face–core–face) or a single layer. The FCF ratio was defined as the ratio of the dry weight of the strands. Table 1 gives the conditions of the series of experimental mats for evaluating
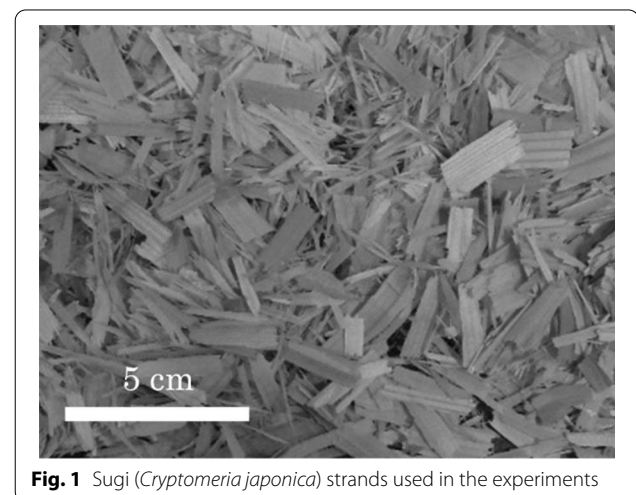

Fig. 1 Sugi (*Cryptomeria japonica*) strands used in the experiments

Murayama *et al. J Wood Sci* (2021) 67:42

Page 3 of 10

Table 1 Series of experimental mats for evaluating the effect of face-layer moisture content (MC)

Face–core–face ratio*	Target moisture content (%)		
	Face-layer	Core-layer	Total
1:2:1	10	10	10.0
1:2:1	12.5	10	11.3
1:2:1	15	10	12.5
<u>1:2:1</u>	<u>20</u>	<u>10</u>	<u>15.0</u>
1:2:1	25	10	17.5
1:2:1	30	10	20.0

* Face–core–face (FCF) ratio was defined as the ratio of the dry weight of the strands contained in the face-layer to the total dry weight of the strands

Underlined mats were also used for evaluating the effect of FCF ratio (see Table 2)

the face-layer MC effect. In this series, the FCF ratio was fixed at 1:2:1 and the face-layer MC was adjusted from 10 to 30%. In another series for evaluating the FCF ratio effect, the face-layer MC was fixed at 20%, and the FCF ratio was varied as shown in Table 2. The MC of the mat core-layer was fixed at 10% except for the 1:0:1 FCF ratio mat, which was a single-layer board. The 10% face-layer MC and 10% core-layer MC mats were treated as three layer boards, because they were conditioned in different plastic bags.

The mat was hot-pressed under the pressure of 3 MPa at the press platen temperature of 180 ℃. The mat thickness was maintained by a pair of bars separated by 10 mm. The target density, dimensions, and MC of the boards were 0.75 g/cm^3, $340 \times 320 \times 10$ mm, and 8%, respectively. Three replicates were produced under each condition. No adhesive was applied, because the aim was to investigate the effect of MC in the mat. Prior to hot-pressing, a temperature and gas pressure sensor (Press-MAN Lite, Alberta Research Council, Alberta, Canada), and the temperature and gas pressure were measured at

Table 2 Series of experimental mats for evaluating the effect of face–core–face (FCF) ratio

Face–core–face ratio*	Target moisture content (%)		
	Face-layer	Core-layer	Total
1:14:1	20	10	11.3
1:6:1	20	10	12.5
<u>1:2:1</u>	<u>20</u>	<u>10</u>	<u>15.0</u>
1:1:1	20	10	16.7
1:0:1	20	–	20.0

* Face–core–face (FCF) ratio was defined as the ratio of the dry weight of the strands contained in the face-layer to the total dry weight of the strands

Underlined mats were also used for evaluating the effect of face-layer MC (see Table 1)

1-s intervals until the core temperature reached 180 ℃. This sensor is a data acquisition system for monitoring internal mat temperature and gas pressure. In this study, since only the mat MC is changed, the main gas pressure is the vapor pressure. Thus, we describe it as vapor pressure, not as gas pressure.

Results and discussion

Effect of face-layer MC on temperature and vapor pressure behavior

Figure 2 shows the typical core temperature–time and vapor pressure–time curves of the mat series with different face-layer MCs. Under all face-layer MC conditions, the core temperature began increasing at approximately 70 s. Between 70 and 150 s, the mat core rapidly rose to over 100 ℃ and thereafter remained constant or decreased. Finally, the core temperature increased to the platen temperature. The core temperature–time curves exhibited the same trend as previous studies [8, 12, 21]. The core-temperature behavior was divisible into three stages: an initial stage of rapid temperature rise, an intermediate stage of limited temperature rise or decrease (here defined as the plateau), and a later stage of temperature rise (see Table 3). During the initial stage, the core temperature at the same hot-pressing time increased
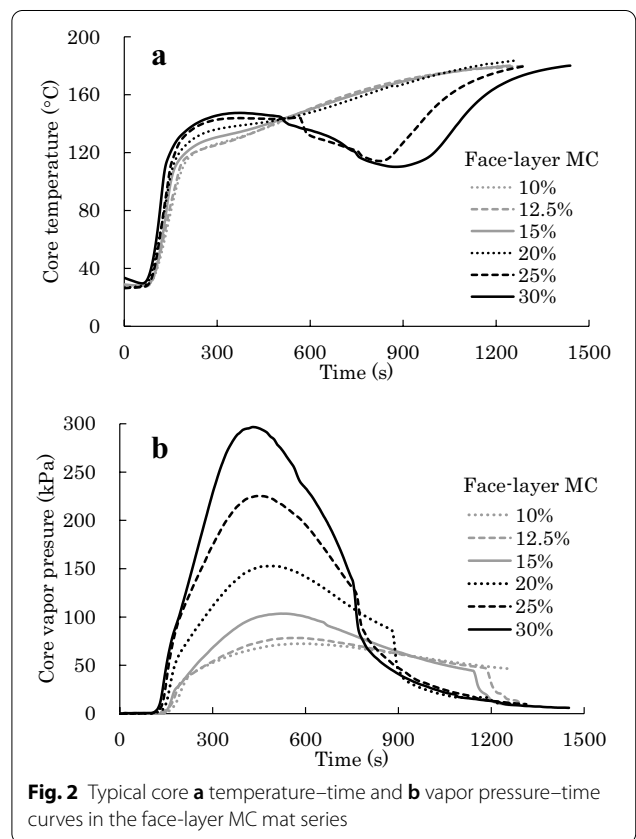

Fig. 2 Typical core **a** temperature–time and **b** vapor pressure–time curves in the face-layer MC mat series

Table 3 Indices of the core temperature–time and vapor pressure–time curves

Index	Definition
t_1	Time at which the core temperature reaches 100 °C (in initial stage)
T_p	Temperature point at which the absolute value of the slopes of the tangential lines at each time point after 100 °C on the temperature–time curve becomes the first local minimum (in intermediate stage)
t_2	Figure 4a: time at which the core temperature is 3% higher than at the last intersection between the tangential line at T_p and the core temperature curve (in intermediate stage)
	Figure 4b: time at which the core temperature is minimized after T_p (in intermediate stage)
t_3	Time at which the core temperature reaches 180 °C (in later stage)
VP_{max}	Maximum core vapor pressure
t_s	Time at which the core vapor pressure starts to increase
t_m	Time at which the core vapor pressure reaches VP_{max}
VP_{rate}	Rate of vapor generation and vapor flow to the mat core, calculated as $VP_{rate} = VP_{max}/(t_m - t_s)$

with face-layer MC. In this stage, vaporization of the surface moisture generated a steep vapor flow that accelerated the convective heat transfer to the mat core [8, 12, 16–18]. The rise in core temperature with face-layer MC can be explained by the enhanced vapor flow increment at high face-layer MC. During the intermediate stage, the core temperature decreased in the mats with face-layer MC ≥ 25% at approximately 300 s, and then the core temperature was lower in these mats than in the mats with face-layer MC < 25% at approximately 600 s. In this stage, the heat energy is mainly consumed for the moisture vaporization, because the temperature inside the mat exceeded the moisture boiling point [16, 18]. Especially, the core temperature decrement was caused by the high-temperature vapor, which rapidly escaped from the mat core to the mat edge. The vapor escape is thought to accelerate at higher vapor pressures. Indeed, the core vapor pressure was higher in the mats with face-layer MC above 25% than in those with lower face-layer MC (Fig. 2b). Thus, the core temperature in this study appeared to decrease when the VP_{max} exceeded 220 kPa. During the later stage, almost all of the moisture had evaporated from the mat, and the core temperature gradually increased through heat conduction from the hot platen. The rise rate of the core temperature increased when the core temperature had decreased in the previous stage (i.e., in the mats with face-layer MC ≥ 25%). This behavior might be explained by the higher temperature gradient between the mat core and hot platen under these conditions, as previously reported [12]. The core vapor pressure of the mat began increasing at approximately 120 s (Fig. 2b), peaked at 400–550 s, and then decreased. Similar vapor pressure behavior was reported in previous studies [17, 21, 22]. The VP_{max} was also enhanced at higher face-layer MC; this result was consistent with previous studies which evaluated the temperature and
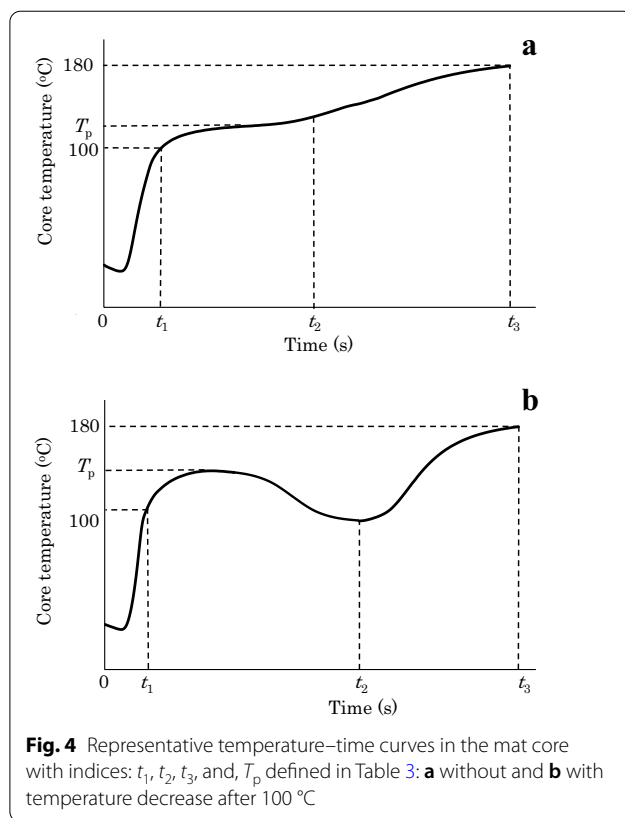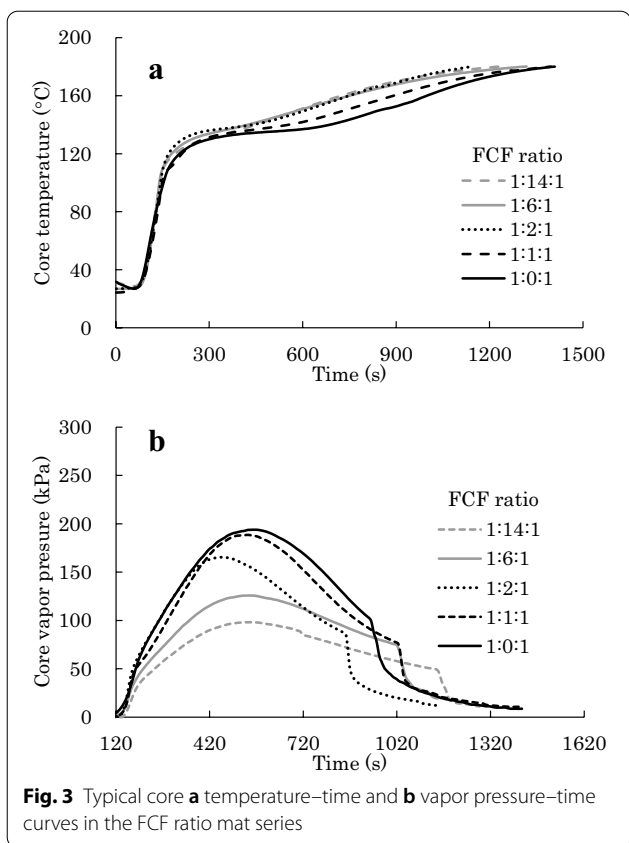
vapor pressure behavior in mats with different MCs but without a moisture gradient [8, 12, 15, 16]. Furthermore, the time t_m to reach VP_{max} decreased with increasing face-layer MC. Increased VP_{max} and lower t_m at higher face-layer MC can be reasonably expected, because more vapor is generated from mats with higher face-layer MC, and a faster vapor flow enters the mat core.

Effect of FCF ratio on temperature and vapor pressure behavior

Figure 3 shows the typical core temperature–time and vapor pressure–time curves of the mat series with different FCF ratios. The core temperature–time curves of the FCF series followed almost the same trends as those of the face-layer MC series, except for the mats with 25 and 30% face-layer MC (Figs. 2a and 3a). After 150 s, 1:0:1 FCF ratio yielded the lowest core temperature at the same hot-pressing time, followed by 1:1:1 FCF ratio and others. The core vapor pressure began increasing at approximately 120 s, peaked around 450–600 s, and then decreased (Fig. 3b). The VP_{max} increased with face-layer thickness. This trend might be explained by the increased MC in mats with higher face-layer thickness. On the other hand, no clear relationship between t_m and FCF series was observed. The VP_{max} trend of FCF series was same as that of face-layer MC series. However, the t_m trend of FCF series was different that of face-layer MC series.

Indices of the temperature–time and vapor pressure–time curves

In the previous subsections, we qualitatively evaluated the core temperatures and vapor pressure behaviors in the mats of the face-layer MC and FCF series. In this subsection, we quantify the relationship between these behaviors and the mat conditions by calculating the time,

Murayama *et al. J Wood Sci*   (2021) 67:42

Page 5 of 10

Fig. 3 Typical core **a** temperature–time and **b** vapor pressure–time curves in the FCF ratio mat series

Fig. 4 Representative temperature–time curves in the mat core with indices: t_1, t_2, t_3, and, T_p defined in Table 3: **a** without and **b** with temperature decrease after 100 °C
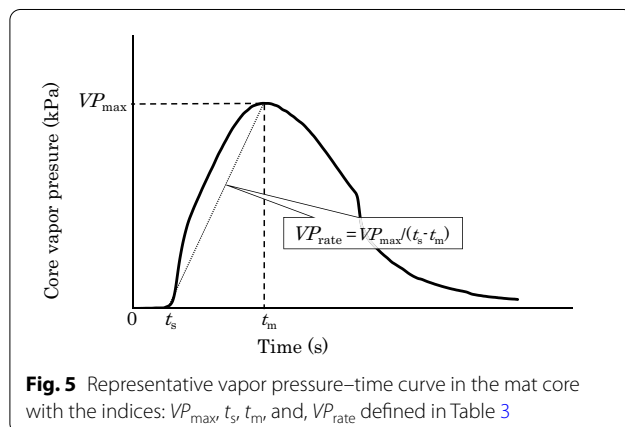
temperature, and vapor pressure indices. The indices of the core temperature–time curve were defined as follows: time to reach 100 °C during the initial stage (t_1), plateau temperature (T_p) and time to complete plateau (t_2) during the intermediate stage, and time to reach 180 °C (t_3) during the later stage. Table 3 lists the indices computed from the core temperature–time and vapor pressure–time curves, and Fig. 4 shows representative temperature–time curves in the mat core with the indices. In core temperature–time curve without temperature decrease after 100 °C (Fig. 4a), to determine T_p and t_2, the tangential lines were set at each time after the temperature reached 100 °C. The slopes of these tangential lines were calculated using the two values at 5 s before and after each time. The core temperature point at which the absolute value of these slopes became the first local minimum was defined as T_p, and the time at which the core temperature was 3% higher than at the last intersection between the tangential line at T_p and the core temperature curve was defined as t_2. When the temperature decreased after 100 °C (Fig. 4b), T_p was defined as described for Fig. 4a, but t_2 was defined as the time of the minimum core temperature after T_p.

Figure 5 shows representative vapor pressure–time curves in the mat core with the indices. The indices of these curves were VP_{max} and the rate of vapor pressure increase VP_{rate}. Here, VP_{rate} defines the rate of vapor generation and vapor flow, and is calculated as:

$$VP_{rate} = \frac{VP_{max}}{t_m - t_s}, \tag{1}$$

where t_s is the time at which the vapor pressure begins increasing.

Fig. 5 Representative vapor pressure–time curve in the mat core with the indices: VP_{max}, t_s, t_m, and, VP_{rate} defined in Table 3

Murayama *et al. J Wood Sci*   (2021) 67:42

Page 6 of 10

Quantitative evaluation of temperature–time and vapor pressure–time curves

This subsection investigates the relationship between the average values of the above-defined indices and the measured total MCs in the series with different face-layer MCs and FCF ratios. In the face-layer MC series, the measured total MCs of the mats with 10, 12.5, 15, 20, 25, and 30% face-layer MC were 10.6, 11.7, 12.2, 15.0, 17.5, and 20.2%, respectively. In the FCF series, the measured total MCs of the mats with 1:14:1, 1:6:1, 1:2:1, 1:1:1, 1:0:1 FCF ratio were 12.1, 13.0, 15.0, 17.1, and 19.3%, respectively. In 19.3% total MC of FCF series, the average value of time indices (t_1–t_3) was calculated by two samples because the measuring start of one of this series mats was a little delayed. On the other hand, vapor pressure and temperature indices of 19.3% total MC of FCF series were calculated by three samples since we could measure these data correctly.

Figure 6 shows the relationships between t_1 and total MC in the face-layer MC and FCF series. In the face-layer MC series, shorter t_1 resulted in higher total MC. Similar results were reported in previous studies of the temperature behavior in mats with no vertical moisture gradient [8, 12, 15, 16]. The reason for this result might be that the convective heat transfer at mat core increased due to the vapor flow from the mat surfaces. Furthermore, the relationship between t_1 of face-layer MC series and total MC was expressed by a negative linear regression with correlation coefficient (R) of 0.98. In the FCF series, the relationship between t_1 of face-layer MC series and total MC was expressed by a positive linear regression with R of 0.97. This trend clearly differed from those of different MC mats without a moisture gradient [8, 12, 15, 16]. Comparing the trends of the face-layer MC and FCF series, we observed that

t_1 was shorter (longer) in the FCF series than in the face-layer MC series at total MCs below (above) 15%. At total MCs below 15%, the FCF series presented higher face-layer MC and lower face-layer thickness than the face-layer MC series (Table 1). Conversely, at total MCs above 15%, the FCF series presented lower face-layer MC and higher face-layer thickness than the face-layer MC series (Table 2). These results suggest that t_1 is shortened in mats with higher face-layer MC and lower face-layer thickness.

Figure 7 plots the relationships between VP_{rate} and total MC of the mats in the face-layer MC and FCF series. In the face-layer MC series, VP_{rate} and total MC were strongly positively related ($R = 0.99$). In mats with higher total MC, the VP_{rate} increase can be explained by the increased vapor flow from the mat surfaces. This assumption consolidates the relationship between t_1 and total MC in the face-layer MC series (Fig. 6). In the FCF series, the VP_{rate} increased while the total MC was below 15%, and converged above 15% total MC (the mat with 1:2:1 FCF ratio). Hence, the generation and rate of vapor flow increased up to 50% face-layer thickness, although the face-layer MC of this series was fixed at 20%. Meanwhile, t_1 increased with total MC (Fig. 6). t_1 increased with face-layer thickness even though VP_{rate} did not rise in the condition above 50% face-layer thickness. This result suggests that t_1 increases even though vapor generation and vapor flow do not rise. Therefore, it is thought that t_1 increases as a result of the heat absorption due to vaporization and the heat transfer of the wood because of the change in the mats FCF ratio. The VP_{rate}s of the face-layer MC and FCF series were almost identical up to 15% total MC, but above 15% total MC, the VP_{rate} was higher in the FCF series than in the face-layer MC series. This result suggests that the
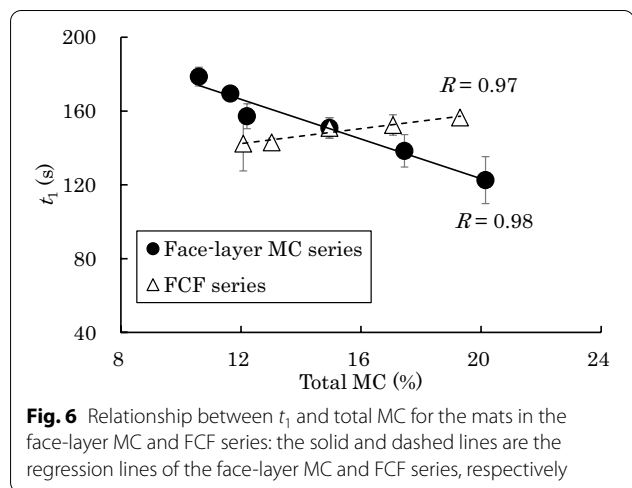
Fig. 6 Relationship between t_1 and total MC for the mats in the face-layer MC and FCF series: the solid and dashed lines are the regression lines of the face-layer MC and FCF series, respectively
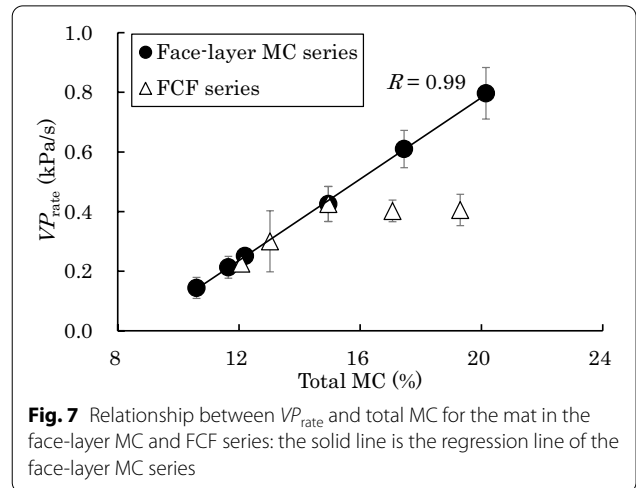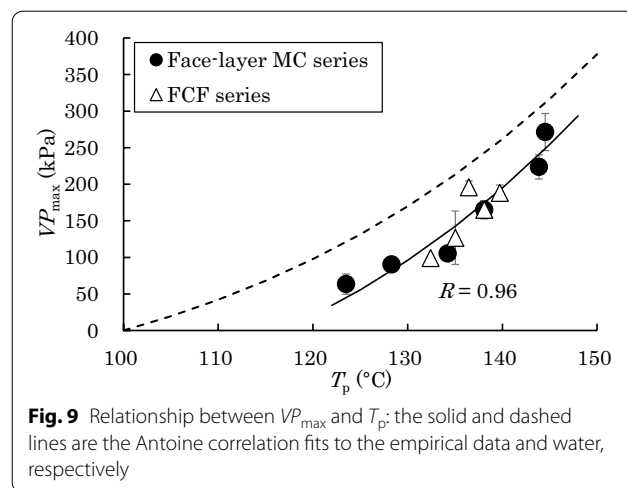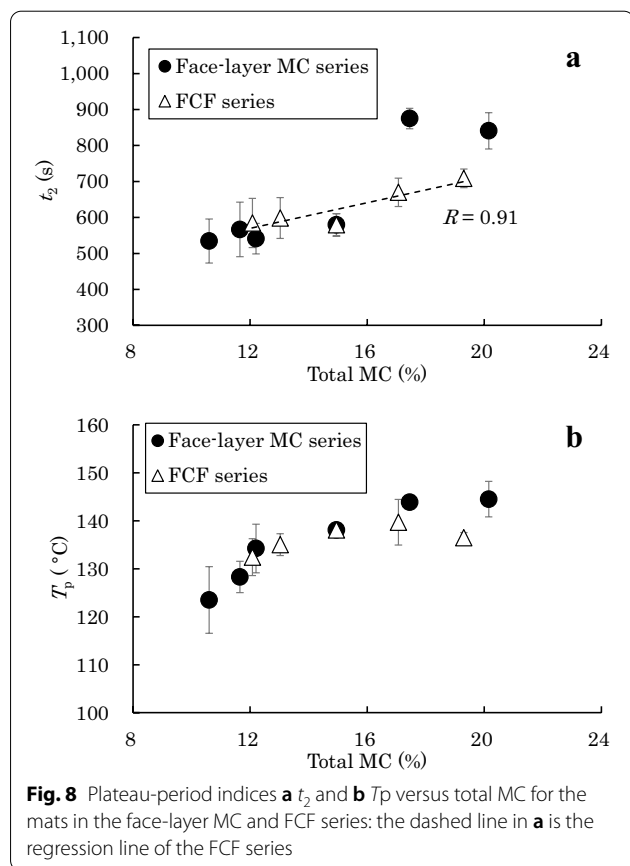
Fig. 7 Relationship between VP_{rate} and total MC for the mat in the face-layer MC and FCF series: the solid line is the regression line of the face-layer MC series

difference between face-layer MC and FCF ratio did not affect the vapor generation and flow in the mats with total MC ≤ 15%.

Figure 8 shows the relationships between the intermediate-stage plateau period and total MC of the mats in the face-layer MC and FCF series. In the face-layer MC series, t_2 increased only when the total MC was 17.5% or lower; otherwise, it was insensitive to total MC. In the FCF series, t_2 linearly increased with total MC ($R = 0.91$). At total MCs of 15% or lower, the relationships between t_2 and total MC exhibited almost the same trends in the two series. Above 15% total MC, t_2 was longer in the face-layer MC series than in the FCF series. Note that at total MCs above 17.5%, the t_2 indices in the mats of the face-layer MC series cannot be compared because they are defined in different ways. Meanwhile, the T_p in the face-layer MC series increased up to 17.5% total MC, and converged at total MCs of 17.5% and higher (Fig. 8b). As the VP_{rate} in the face-layer MC series linearly increased with total MC (Fig. 7), it was assumed that convective heat transfer derived from the vapor flow was accelerated at 17.5% and higher total MCs. Conversely, the high-temperature vapor may rapidly escape from the mat interior, because the core temperatures in the mats

of the face-layer MC series reduced when the total MC was 17.5% or higher (25% face-layer MC in Fig. 2a). It was assumed that vapor escape did not increase the T_p, but the effect of vapor escape was difficult to evaluate in this study. In future work, the vapor pressure behavior outside the mat core must be investigated along a vertical MC gradient. In the FCF series, T_p increased at total MCs of 15% (the mat with 1:2:1 FCF ratio) or lower, and became constant at higher 15% total MC (Fig. 8b). The VP_{rate} of the FCF series mats followed a similar trend (Fig. 7). At total MCs up to 15%, the T_p trends were almost identical in the face-layer MC and FCF series, but above 15% total MC, the T_p was higher in the face-layer MC series than in the FCF series. Despite their higher T_p, mats with total MCs of 17.5% and higher (the mat with 25% face-layer MC) in the face-layer MC series required a longer t_2. A higher T_p accelerates the resin curing and plasticization of wood in the core-layer, thus increasing the internal bonding in the mat [5, 14]. This result suggests that mats fabricated at higher T_p enhance the mechanical properties of the boards. Thus, it is thought the mats with higher T_p become the high mechanical properties boards in this study. However, the longer t_2 indicates a lower productivity at higher T_p. There is also a possibility that T_p changes due to the adhesive effect when the adhesive is added. To understand how the temperature and vapor pressure behaviors affect the productivity, the mats must be bonded with adhesives and evaluated under different press conditions. The effects of adhesive curing and press condition will be considered in future studies.

When evaluating the relationship between T_p and vapor pressure, the VP_{max} was strongly related to T_p in both the face-layer MC and FCF series (Fig. 9). Rofii et al. [21] reported that the empirical correlation between VP_{max} and T_p fits the Antoine equation, which

Fig. 8 Plateau-period indices **a** t_2 and **b** Tp versus total MC for the mats in the face-layer MC and FCF series: the dashed line in **a** is the regression line of the FCF series

Fig. 9 Relationship between VP_{max} and T_p: the solid and dashed lines are the Antoine correlation fits to the empirical data and water, respectively

Murayama *et al. J Wood Sci* (2021) 67:42

Page 8 of 10

empirically models the vapor pressure P as a function of temperature T:

$$P = 10^{\left(A - \frac{B}{T+C}\right)}. \tag{2}$$

In this expression, A, B, and C are constants that must be derived from experimental vapor pressure and temperature. When fitted to the Antoine equation, the relationship between VP_{max} and T_p yielded A, B, and C values of 5.69, 334.19, and 2.55, respectively. This relationship was highly correlated ($R = 0.96$). Therefore, it is thought that the relationship between VP_{max} and T_p can be approximated by the Antoine equation, regardless of the difference of face-layer MC and FCF ratio among mats. For pure steam, A, B, and C are 8.03, 1705.62, and 231.41, respectively [23] (Fig. 9). In this study, a higher core temperature was achieved under lower core vapor pressure than in pure steam. In a previous study [21], the relationship between the intermediate-stage temperature and VP_{max} of the mats which have different densities and furnish types followed the Antoine equation of pure steam. On the other hand, in the earlier studies, the vapor pressure in the flake-based different total MC mats was lower than the vapor pressure obtained from the temperature and pressure relationship of pure steam [10]. It is a well-known fact that correlation lines illustrated by the Antoine equation almost overlap that by the temperature and pressure relationship of pure steam. The tendencies of the earlier studies [10, 13] were reflected in the present study. Kamke and Casey [10] posited that the adsorbed water molecules in wood exhibit a lower vapor pressure than pure steam. The mat permeability is also reportedly related to the temperature and vapor pressure behavior [12]. The permeability is thought to change in mats with high face-layer MC because the mat faces densify by the high hydrothermal effect of wooden materials. Moreover, the heat characteristics of wood which are varied by species and densities probably affect the core temperature behavior of the mat. To clarify these effects and better understand the relationship between temperature and vapor pressure inside the mat, we require the continuous accumulation of relevant experimental data.

Figure 10 shows the relationships between t_3 and total MC in the face-layer MC and FCF ratio mat series. The t_3 decreased in the mats with total MC contents of 15% or higher (20% face-layer MC with 1:2:1 FCF ratio), and then increased in both series. In mats with lower MC, the temperature is gradually elevated because wood is a poor heat conductor and the convective heat transfer of vapor is a little [8, 12, 15, 16]. Conversely, in mats with extremely high MC, the temperature increase is restrained because a large amount of heat is devoted to
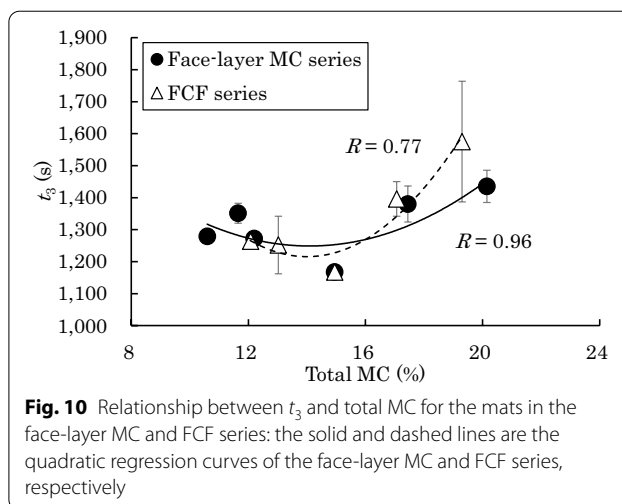

Fig. 10 Relationship between t_3 and total MC for the mats in the face-layer MC and FCF series: the solid and dashed lines are the quadratic regression curves of the face-layer MC and FCF series, respectively

water vaporization from the mat. Therefore, an optimum MC condition of the mats is expected. The mat core behavior at t_3 suggests that the 20% face-layer MC mat with 1:2:1 FCF ratio optimizes the effect of heat transfer which includes the heat conduction from the hot platen, convective heat transfer derived from vapor flow, heat absorption caused by vaporization, and the heat transfer of wood, in this study. When comparing t_3 of face-layer MC and FCF series, the difference was not observed at 17.5% total MC or lower. On the other hand, at the highest total MC in both series, t_3 was longer in the FCF series than in the face-layer MC series, even though the t_3 at the highest total MC of FCF series had a large variation. In the high total MC, it is thought that core moisture requires a longer vaporization time than surface moisture does. In a quadratic regression between t_3 and total MC, the correlation coefficients of the face-layer MC and FCF series were 0.77 and 0.92, respectively.

The relationship between total MC and t_1 differed between the FCF ratio and face-layer MC series, but the relationships between total MC and VP_{rate}, t_2, T_p, and t_3 trended similarly in both series (except when the core temperature decreased over the face-layer MC series). In the absence of a core temperature decrease, these results suggest that the effects of FCF ratio and face-layer MC differ only by the convective heat transfer derived from vapor flow in the initial stage differed. In future work, we must evaluate the effects of the moisture gradient in mats with higher face-layer MC and thinner surfaces than those prepared for this study.

Conclusions

This study evaluated the effects of face-layer MC and FCF ratio on the core temperature and vapor pressure behaviors of mats for wood-based panels during

Murayama *et al. J Wood Sci*   (2021) 67:42

Page 9 of 10

hot-pressing. Specifically, we quantified the indices of the core temperature–time curves and vapor pressure–time curves of the face-layer MC and FCF series, and investigated the relationship between each index and the total MC. These results suggest that the effect of face-layer MC and FCF ratio only differ by the convective heat transfer derived from vapor flow in the initial stage unless the core temperature decrement does not occur. The main results of this study are summarized below:

1) The index t_1 in the initial stage (the rapid temperature-rise stage) decreased at higher face-layer MC and increased at higher FCF ratio. This index is expected to be shortened in mats with higher face-layer MC and lower FCF ratio.
2) The index T_p in the intermediate stage (when the temperature plateaued) was increased in the mats with total MCs of 17.5% or higher (the mat with 25% face-layer MC) in the face-layer MC series, but these mats required a longer t_2 than the other mats.
3) The T_p and VP_{max} were strongly related in both the face-layer MC and FCF series. This relationship was well expressed by the Antoine equation with appropriate constants derived from the data.
4) The index t_3 in the later stage (when the temperature rose again) decreased in mats with total MCs of 15% or lower (20% face-layer MC with 1:2:1 FCF ratio), and increased with total MC in both series. The 20% face-layer MC mat with 1:2:1 FCF ratio may have optimized the heat transfer in this study.

The presented results are expected to enhance our understanding of the heat and mass transfers during hot-pressing, and are useful to improve the manufacturing process of wood-based panels.

Abbreviations
MC: Moisture content; FCF: Face–core–face; t_1: Time to reach 100 °C in mat core; t_2: Time to complete limited temperature rise or decrease (defined as plateau in this study); t_3: Time when core temperature reaches the platen temperature; T_p: Plateau temperature in the mat core; VP_{max}: Maximum vapor pressure in the mat core; t_s: Time when core vapor pressure starts to increase; t_m: Time when core vapor pressure reaches VP_{max}; VP_{rate}: The rate of core vapor pressure increase.

Authors' contributions
The first and corresponding author participated sufficiently in the work to take public responsibility for the entire contents of the manuscript. The co-authors participated sufficiently in the work to take public responsibility for part of the contents of the manuscript. All authors read and approved the final manuscript.

Availability of data and materials
Not applicable.

Declarations

Ethics approval and consent to participate
Not applicable.

Consent for publication
Not applicable.

Competing interests
The authors declare that they have no competing interests.

Author details
[1]Forestry and Forest Products Research Institute, 1 Matsunosato, Tsukuba, Ibaraki 305-8687, Japan. [2]Faculty of Agriculture, Shizuoka University, 836 Ohya, Suruga-ku, Shizuoka 422-8529, Japan. [3]Shizuoka Professional University of Agriculture, Tomigaoka 678-1, Iwata-city, Shizuoka-ken 438-8577, Japan.

References
1. Dai C, Steiner PR (1993) Compression behavior of randomly-formed wood flake mats. Wood Fiber Sci 25(4):349–358
2. Zhou C, DaiSmith CG (2008) A generalized mat consolidation model for wood composites. Holzforschung 62:201–208. https://doi.org/10.1515/HF.2008.053
3. Dai C, Tu C, Hubert P (2000) Modeling Vertical Density Profile in Wood Composite Boards. In: Proceedings of the 5th Pacific Rim Bio-based Composites Symposium, Canberra, Australia, 10–14 December 2000
4. Zhou C, Smith G, Dai C (2010) Characterizing hydro-thermal compression behavior of aspen wood strands. Holzforschung 63:609–617. https://doi.org/10.1515/HF.2009.111
5. Dai C, Yu C, Zhou C (2007) Theoretical modeling of bonding characteristics and performance of wood composites: part 1. Inter-element contact. Wood Fiber Sci 39(1):48–55
6. Dai C, Yu C, Jin J (2008) Theoretical modeling of bonding characteristics and performance of wood composites: Part IV. Internal bond strength. Wood Fiber Sci 40(2):146–160
7. Wang BJ, Ellis S, Dai C (2006) Veneer surface roughness and compressibility pertaining to plywood/LVL manufacturing. Part II. Optimum panel densification. Wood Fiber Sci 38(4):727–735
8. Wu J, Yu Z, Chen T (2006) Heat-transfer process during hot-pressing of flakeboard. Front For China 3:343–347. https://doi.org/10.1007/s11461_006_0007_7
9. Bolton AJ, Humphrey PE (1988) The hot pressing of dry-formed wood-based composites-part I. A review of the literature, identifying the primary physical processes and the nature of their interaction. Holzforschung 42(6):403–406. https://doi.org/10.1515/hfsg.1988.42.6.403
10. Kamke FA, Casey LJ (1988) Gas pressure and temperature in the mat during flakeboard manufacture. For Prod J 38(3):41–43
11. Wei P, Rao X, Yang J, Guo Y, Chen H, Zhang Y, Chen S, Deng X, Wang Z (2016) Hot pressing of wood-based composites: a review. For Prod J 66(7–8):419–427. https://doi.org/10.13073/FPJ_D_15_00047
12. Rofii MN, Yamamoto N, Ueda S, Kojima Y, Suzuki S (2014) The temperature behaviour inside the mat of wood-based panel during hot pressing under various manufacturing conditions. J Wood Sci 60(6):414–420. https://doi.org/10.1007/s10086_014_1418_y
13. Zombori BG, Kamke FA, Watson LT (2003) Simulation of the internal conditions during the hot-pressing process. Wood Fiber Sci 35(1):2–23

Murayama *et al. J Wood Sci*   (2021) 67:42

Page 10 of 10

14. Dai C, Yu C (2004) Heat and mass transfer in wood composite panels during hot-pressing: part I. A physical-mathematical model. Wood Fiber Sci 36(34):585–597

15. Garcia RA, Cloutier A (2004) Characterization of heat and mass transfer in the mat during the hot pressing of MDF panels. Wood Fiber Sci 37(1):23–41

16. Bolton AJ, Humphrey PE, Kavvouras PK (1988) The hot pressing of dry-formed wood-based composites—part III. Predicted vapour pressure and temperature variation with time, compared with experimental data for laboratory boards. Holzforschung 43(4):265–274. https://doi.org/10.1515/hfsg.1989.43.4.265

17. Garcia PJ, Avramidis S, Lam F (2001) Internal temperature and pressure responses to flake alignment during hot-pressing. Holz Roh Werkst 59:272–275. https://doi.org/10.1007/s001070100218

18. Garcia PJ, Avramidis S, Lam F (2003) Horizontal gas pressure and temperature distribution responses to OSB flake alignment during hot-pressing. Holz Roh Werkst 61:425–431. https://doi.org/10.1007/s00107_003_0411_8

19. Dai C, Yu C, Xu C, He G (2007) Heat and mass transfer in wood composite panels during hot pressing: part 4. Experimental investigation and model validation. Holzforschung 61(1):83–88. https://doi.org/10.1515/HF.2007.013

20. Hata T, Subiyanto B, Kawai S, Sasaki H (1989) Production of particleboard with steam-injection part 1: temperature behavior in particle mat during hot pressing and steam-injection. Wood Sci Technol 23:361–369. https://doi.org/10.1007/BF00353252

21. Rofii MN, Kubota S, Kobori H, Kojima Y, Suzuki S (2016) Furnish type and mat density effects on temperature and vapor pressure of wood-based panels during hot pressing. J Wood Sci 62:163–173. https://doi.org/10.1007/s10086_015_1531_6

22. Humphrey PE, Bolton AJ (1989) The hot pressing of dry-formed wood-based composites—part V. The effect of board size: comparability of laboratory and industrial pressing. Holzforschung 43(6):401–405. https://doi.org/10.1515/hfsg.1989.43.6.401

23. Hirata M, Ohe S, Nagahama K (1975) Computer aided data book of vaor-liquid quilibria. Kodansha, Japan

Publisher's Note

Springer Nature remains neutral with regard to jurisdictional claims in published maps and institutional affiliations.